Available online at www.sciencedirect.com
SCIENCE DIRECT®
Physica E 27 (2005) 469–473
PHYSICA E
www.elsevier.com/locate/physe

Surface-enhanced resonant Raman spectroscopy (SERRS) of single-walled carbon nanotubes absorbed on the Ag-coated anodic aluminum oxide (AAO) surface

X.Y. Dou[a,b], Z.P. Zhou[a,b], P.H. Tan[c], L. Song[a,b], L.F. Liu[a,b], X.W. Zhao[a,b], S.D. Luo[a,b], X.Q. Yan[a,b], D.F. Liu[a,b], J.X. Wang[a,b], Y. Gao[a,b], Z.X. Zhang[a,b], H.J. Yuan[a,b], W.Y. Zhou[a,b], S.S. Xie[a,b,*]

[a]*Institute of Physics, Center for Condensed Matter Physics, Chinese Academy of Sciences, Beijing 100080, PR China*
[b]*Graduate School of the Chinese Academy of Sciences, Beijing 100080, PR China*
[c]*State Key Laboratory for Superlattices and Microstructures, Institute of Semiconductors Chinese Academy of Sciences, Beijing 100083, PR China*

Received 6 January 2005; accepted 10 January 2005
Available online 23 March 2005

Abstract

In this paper, we developed a new kind of substrate, the silver-coated anodic aluminum oxide (AAO), to investigate the characters of surface-enhanced resonant Raman scattering (SERRS) of the dilute single-walled carbon nanotubes. Homogeneous Ag-coated AAO substrate was obtained by decomposing the $AgNO_3$ on the surface of AAO. single-walled carbon nanotubes (SWNTs) were directly grown onto this substrate through floating catalyst chemical vapor deposition method (CVD). SERRS of SWNTs was carried out using several different wavelength lasers. The bands coming from metallic SWNTs were significantly enhanced. The two SERRS mechanisms, the "electromagnetic" and "chemical" mechanism, were mainly responsible for the experiment results.

PACS: 78.30.Na; 78.30.−j; 68.35.−p

Keywords: Single-walled carbon nanotubes (SWNTS); Surface-enhanced resonant raman scattering (SERRS); Anodic aluminum oxide (AAO)

1. Introduction

Since the first report of surface-enhanced Fourier transform Raman spectroscopy on the investigation of Single-walled carbon nanotubes

*Corresponding author. Institute of Physics, Center for Condensed Matter Physics, Chinese Academy of Sciences, Beijing 100080, PR China. Tel.: +86 10 826 490 81; fax: +86 10 826 40 215.
E-mail addresses: xydou@aphy.iphy.ac.cn (X.Y. Dou), ssxie@aphy.iphy.ac.cn (S.S. Xie).

1386-9477/$ - see front matter © 2005 Elsevier B.V. All rights reserved.
doi:10.1016/j.physe.2005.01.009

(SWNTs) deposited on rough gold and silver surfaces [1], many scientists have devoted to search for different materials to get more information of the surface-enhanced resonant Raman scattering (SERRS) of SWNTs [2–5]. Kneipp et al. prepared a silver colloidal cluster solution containing SWNTs in a low concentration and evaporated it onto a microscopic cover slide. They obtained surface enhancement factors of at least 10^{12}. The highly enhanced spectra were observed only at the point in a good contact with the silver particles alone the bundle [2]. Silver/gold island films, colloidal silver clusters on the glass slides and the silver-coated porous silicon were also found to be good candidates for the SERRS substrates [3–5]. In most of these experiments before the isolated nanotubes available, SWNTs were treated with a relatively complex process, such as purification, centrifugation, ultrasonication. The substrates are materials such as glass and silicon. Here, we provide a new substrate, the Ag-coated anodic aluminum oxide (AAO). SWNTs were directly deposited on it through floating catalyst chemical vapor deposition method (CVD). The hexagonal structure of AAO and its walls provide an excellent background for the silver nanoparticles to stick on. Highly enhanced Raman scattering of SWNTs were detected under several different laser wavelengths.

2. Experimental details

The AAO was purchased from Whatman company. The AAO is open at both ends. We first cut down some small slides (5 mm × 5 mm) and adhered onto the silicon wafer at the same size in order to protect the AAO from rupturing. Only one side of the AAO was exposed. Then we used a similar way described in the literature [4]. 1M $AgNO_3$ solution was dropped on the surface of the AAO, in this process only a thin layer of $AgNO_3$ solution was on the AAO surface. Then the solution-covered slide was put into the bake oven at a steady temperature of 110 °C. It was delivered into the temperature-controlled furnace when the slide was completely dried in about 15 min. The slide was kept in the furnace at 450 °C for 20 min and then cooled down to room temperature in the argon current. Thus the Ag-coated AAO on the silicon wafer was acquired, which can be seen through the SEM figures.

The synthesis of SWNTs on this special kind of substrate was through floating catalyst chemical vapor deposition (CVD) in a double-furnace system, as that investigated in Zhoup's paper [6]. In general, the temperatures of the first and second furnace were 58 and 1100 °C, respectively. The catalyst mixture of ferrocene and sulfur was put in first furnace. The carbon source was methane CH_4 (10 sccm) and acetylene C_2H_2 (1.0 sccm) mixture, which were carried by argon flow (1000 sccm). The Ag-coated AAO on silicon wafers was put in the later part of the quartz tube reactor. Grown SWNTs were carried by the argon flow and adsorbed onto the substrate surface. The reaction maintained about 15 min.

We put the product under the SEM to investigate the structure of the SWNTs on the Ag-coated AAO. The SERRS experiments using a T6400 Raman spectrometer under several different wavelengths were carried out using a back scattering configuration under the room temperature.

3. Results and discussion

As we know, AAO usually exhibits hexagonally nanoscale packed cells [7,8]. When we drop the $AgNO_3$ solution on the surface of AAO, the solution can be spread on the ridges and the pores of AAO. After the solution was dried in the bake oven, the $AgNO_3$ formed tiny polycrystals on the surface and in the pores of AAO uniquely. When heated in the controlled furnace,the polycrystals of $AgNO_3$ were decomposed in this way [4]:

$$AgNO_3 \rightarrow Ag(s) + NO_2 \uparrow + (1/2)O_2 \uparrow$$

Silver nanoparticles formed in the pores and on the surface of AAO. Different shapes of silver particles were connected to each other on the surface and formed a rough Ag-coated structure. Fig. 1a shows the typical SEM images of SWNTs on the Ag-coated surface of AAO, from which, we can see the density of the SWNTs is very low, less

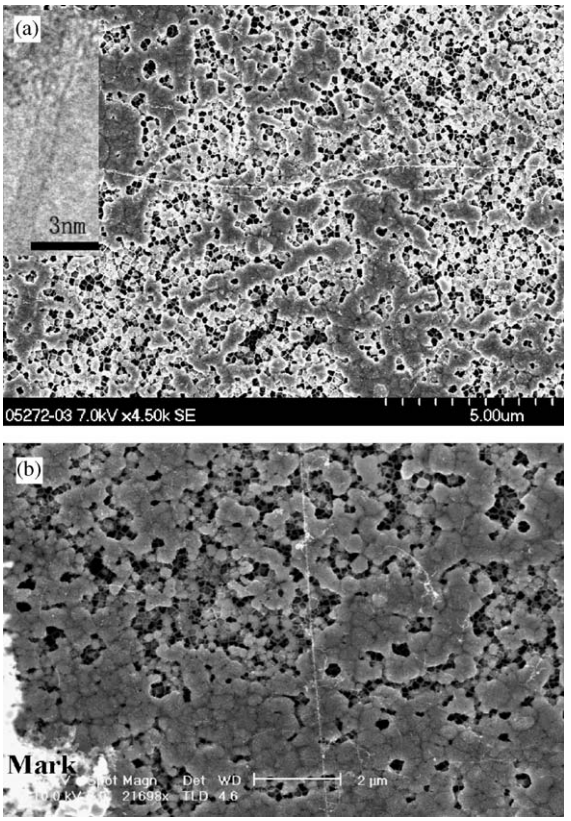

Fig. 1. (a) A typical SEM picture of a SWNTs bundle on the Ag-coated AAO substrate, the inset was the HRTEM of a SWNT directly deposited on the copper grid. (b) SEM picture of the marked SWNTs on which the SERRS experiments were performed.

than 1 nanotube or its bundle per μm^2. In most area of the slide the silver particles were in a disordered arrangement on AAO surface. They had an average size of 1–200 nm. Many silver particles are connected to each other on AAO surface, perhaps due to the high concentration of $AgNO_3$ in the solution. Some uncovered pores of AAO can also be clearly seen. In this way, the silver formed a network that provided an efficient structure for SERRS of SWNTs. HRTEM of SWNTs on a copper grid obtained at the same time was also shown in Fig. 1. From the TEM picture, we found that some SWNTs formed bundles and some were in single status. A small mark was made on the substrate to indicate the position of the designated SWNTs under both SEM and Raman microscope (Fig. 1b).

In Fig. 2a, SERRS of SWNTs using 488 nm (2.54 eV) wavelength laser was shown. RBM mode

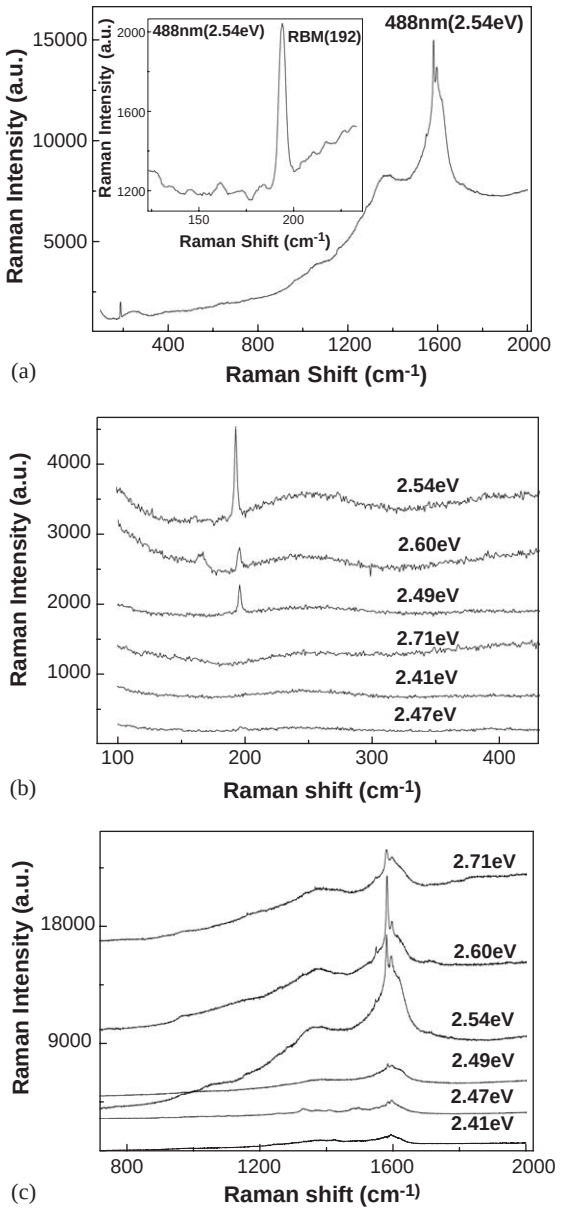

Fig. 2. (a) SERRS spectra of SWNTs on the Ag-coated AAO substrate under 488 (2.54 eV), the inset was the RBM band at 192 cm^{-1}. (b) RBM and (c) G-band under different laser excitation wavelengths.

at 192 cm^{-1} resonant with the incident E_{laser} can be identified from a semiconducting SWNT within the small bundle [9–11]. Its diameter could be calculated to be 1.3 nm from the equation $d = \alpha/\omega_{RBM}$ (here $\alpha = 248\,cm^{-1}\,nm$) [12,13]. We noticed that signals above 1000 cm^{-1} were elevated significantly. It was due to photoluminescence of AAO substrate. D-band at about 1350 cm^{-1}, which comes from some amorphous carbon adsorbed on SWNTs and double resonant Raman scattering mechanism [14], was also greatly enhanced. The shape of D-band was changed compared with that of the normal Raman scattering of SWNTs because of the effect of the substrate. G-band of this small bundle can be identified as a combine of both semiconducting and metallic SWNTs. The peaks at 1545, 1580, 1592, 1615 cm^{-1} were all clearly seen in the spectra. We noticed that the peak at 1580 cm^{-1} from metallic SWNTs was significantly enhanced exhibiting a much stronger signal than that at 1592 cm^{-1} from semiconducting SWNTs [15]. We attribute this to that the electromagnetic and the chemical interactions between the silver particles and the metallic SWNTs were much stronger than those between the silver particles and the semiconducting SWNTs.

Fig. 2b gave the RBM band of the SWNTs bundle marked on the substrate under different laser energies from 2.41 to 2.71 eV. The resonant intensity at 192 cm^{-1} under 488 nm (2.54 eV) incident laser was much stronger than that under the other ones. It is due to that the electronic transition E_{33} of the specific semiconducting SWNT within the bundle is corresponding to the incident photon energy E_{laser} at 488 nm [11]. The Resonant intensity under 496.5 nm (2.49 eV) and 476.5 nm (2.60 eV) were much lower than that under 488 nm (2.54 eV). That RBM signal was much weaker under 2.47 eV, and even could not be detected under a much lower energy (2.41 eV) or a higher energy (2.71 eV). This could be explained by the fact that the energy band gap (E_{ii}) of SWNTs has a resonant window with the incident laser [10,11].

Fig. 2c shows the typical enhanced G-band of the same bundle under different laser excitation wavelengths. In the normal Raman scattering, due to the small concentration (about 1/3) of the metallic SWNTs in the film samples or in the large bundles, the signal at 1580 cm^{-1} is much lower than that at 1592 cm^{-1}. However, SERRS signal at 1580 cm^{-1} can be so greatly enhanced that it can be compared with that at 1592 cm^{-1}. Furthermore, the peak at 1592 cm^{-1} in SERRS was almost the same as that in normal resonant Raman scattering under different laser wavelengths. But the peaks at 1580 and 1545 cm^{-1}, which originate from the metallic SWNTs, were enhanced under different wavelengths compared with the normal resonant Raman scattering signals [3]. From Fig. 2c, we notice the signals at 1580 cm^{-1} under 2.60 and 2.54 eV were much stronger than that under lower energies of 2.41, 2.47, 2.49 eV and higher energy 2.71 eV. We infer that in the single bundle we explored in the experiments the metallic SWNTs have small diameters at around 0.9 nm (E_{11} resonant with E_{laser}) or large diameters at around 1.8 nm (E_{22} resonant with E_{laser}). The other important feather in the enhanced signals was that the full-width at half-maximum intensity (Γ) at 1580 cm^{-1} was very small under different laser wavelengths (shown in Table 1). The relative intensity I/I_{1592} under each laser wavelength was introduced to character the enhanced degree for the other Raman peaks. We could see that the relative intensity I_{1580}/I_{1592} reached the maximum value 3.0 when $E_{laser} = 2.60$ eV.

The reason of SERRS for the metallic SWNTs comes from the good contact between the bundle and the special surface structure of silver-coated AAO. As we all know that the AAO usually exhibits a special self-ordered structure in which nanometer scaled pores occur in the center of hexagonally packed cells. The silver particles adhered in the pores and on the ridges of AAO substrate. Although the origin of SERRS are still under investigation, there are mainly two supporting theories [16–18]: (1) ''electromagnetic'' mechanism that is due to the enhanced electromagnetic fields at or near the nanometer size metallic particles, (2) ''chemical'' mechanism that comes from the charge transfer between the metallic surface and the SWNTs. Both the mechanisms were responsible for the enhanced Raman scattering in our experiments.

Table 1
Raman shift (ω), relative Raman intensity (I/I_{1592}) of each Lorentzian component for G-band and the full width at half maximum intensity (Γ) under different laser excitation wavelengths

ω (cm^{-1})		514.5 nm (2.41 eV)	501.7 nm (2.47 eV)	496.5 nm (2.49 eV)	488 nm (2.54 eV)	476.5 nm (2.60 eV)	457.9 nm (2.71 eV)
1545	I/I_{1592}	1.5	1.2	2.0	0.9	0.6	0.5
	Γ (cm^{-1})	116	119	99	81	36	42
1580	I/I_{1592}	0.7	0.6	0.8	1.4	3.0	1.7
	Γ (cm^{-1})	46	5	5	7	7	11
1592	I/I_{1592}	1.0	1.0	1.0	1.0	1.0	1.0
	Γ (cm^{-1})	26	10	19	19	14	23
1615	I/I_{1592}	0.8	1.5	1.3	1.1	1.3	1.3
	Γ (cm^{-1})	39	66	37	39	57	67

4. Conclusions

In summary, we have developed a new substrate, Ag-coated AAO, to investigate the SERRS of SWNTs under several near ultraviolet laser excitation wavelengths. We found the several peaks of G-band of the Raman signal from metallic SWNTs were significantly enhanced. The resonance energy was corresponding to the electronic transition of SWNTs. We believe that special structure of the Ag-coated AAO provided a main reason for the enhanced Raman signals in the experiments.

Acknowledgments

We thank C.Y. Wang for her assistance in SEM work, K. Zhu for her assistance in the Raman experiments. This work is financially supported by the National Natural Science Foundation of China "One-dementional nano scale materials".

References

[1] S. Lefrant, I. Baltog, M. Lamy de la Chapelle, M. Baibarac, G. Louarn, C. Journet, P. Bernier, Synth. Met. 100 (1999) 13.
[2] K. Kneipp, P. Corio, S.D.M. Brown, K. Shafer, J. Motz, L.T. Perelman, E.B. Hanlon, A. Marucci, G. Dresselhaus, M.S. Dresselhaus, Phys. Rev. Lett. 84 (2000) 3470.
[3] P. Corio, S.D.M. Brown, A. Marucci, M.A. Pimenta, K. Kneipp, G. Dresselhaus, M.S. Dresselhaus, Phys. Rev. B 61 (2000) 13202.
[4] S. Chan, S. Kwon, T.W. Koo, L.P. Lee, A.A. Berlin, Adv. Mater. 19 (2003) 1595.
[5] S. Lefrant, I. Baltog, M. Baibarac, J. Schreiber, O. Chauvet, Phys. Rev. B 65 (2002) 235401.
[6] Z.P. Zhou, L.J. Ci, L. Song, X.Q. Yan, D.F. Liu, H.J. Yuan, Y. Gao, J.X. Wang, L.F. Liu, W.Y. Zhou, G. Wang, S.S. Xie, Carbon 41 (2003) 2607.
[7] H. Masuda, K. Fukuda, Science 268 (1995) 1466.
[8] H. Masuda, H. Yamada, M. Satoh, H. Asoh, Appl. Phys. Lett. 72 (1997) 2770.
[9] A.M. Rao, E. Richter, S. Bandow, B. Chase, P.C. Eklund, K.A. Williams, S. Fang, K.R. Subbaswamy, M. Menon, A. Thess, R.E. Smalley, G. Dresselhaus, M.S. Dresselhaus, Science 275 (1997) 187.
[10] H. Kataura, Y. Kumazawa, Y. Maniwa, I. Umezu, S. Suzuki, Y. Ohtsuka, Y. Achiba, Synth. Met. 103 (1999) 2555.
[11] R. Saito, G. Dresselhaus, M.S. Dresselhaus, Phys. Rev. B 61 (2000) 2981.
[12] S. Bandow, S. Asaka, Y. Saito, A.M. Rao, L. Grigorian, E. Richter, P.C. Eklund, Phys. Rev. Lett. 80 (1998) 3779.
[13] M. Milnera, J. Kürti, M. Hulman, H. Kuzmany, Phys. Rev. Lett. 84 (2000) 1324.
[14] C. Thomsen, S. Reich, Phys. Rev. Lett. 85 (2000) 5214.
[15] M.A. Pimenta, A. Marucci, S. Empedocles, M. Bawendi, E.B. Hanlon, A.M. Rao, P.C. Eklund, R.E. Smalley, G. Dresselhaus, M.S. Dresselhaus, Phys. Rev. B 58 (1998) 16016.
[16] V.M. Shalaev, M.I. Stockman, Zh. Éksp. Teor. Fiz. Sov. Phys. JETP 65 (1987) 287.
[17] V.A. Markel, V.M. Shalaev, P. Zhang, W. Huynh, L. Tay, T.L. Haslett, M. Moskovits, Phys. Rev. B 59 (1999) 10 903.
[18] M.I. Stockman, V.M. Shalaev, M. Moskovits, R. Botet, T.F. George, Phys. Rev. B 46 (1992) 2821.